Field and frequency dependent transport in the two-dimensional organic conductor α-(BEDT-TTF)2I3

M. Dressel, G. Grüner, Jean Pouget, A. Breining, D. Schweitzer

Classification
Physics Abstracts
72.15N — 78.30J — 78.70C

Field and frequency dependent transport in the two-dimensional organic conductor α-(BEDT-TTF)$_2$I$_3$

M. Dressel ([1]), G. Grüner ([1]), J.P. Pouget ([2]), A. Breining ([3]) and D. Schweitzer ([3])

([1]) Department of Physics and Solid State Science Center, University of California, Los Angeles, CA 90024-1547, U.S.A.
([2]) Laboratoire de Physique des Solides, Universite Paris-Sud, F-91405 Orsay, France
([3]) Drittes Physikalisches Institut, Universität Stuttgart, D-70569 Stuttgart, Germany

(Received 10 October 1993, accepted in final form 3 January 1994)

Abstract. — The title compound undergoes a metal-insulator phase transition of unknown origin at $T_{MI} = 135$ K. We studied the electrodynamic response of α-(BEDT-TTF)$_2$I$_3$ in a wide range of frequency, covering microwave and millimeter wave frequencies as well as the optical spectral range, and found a frequency dependent conductivity up to 1000 cm^{-1} in the low temperature phase. This is accompanied be a non-linear transport with a smooth onset at about 10 V/cm. Our X-ray studies show no indication of superstructure reflections and clearly rule out the formation of a charge density wave ground state. The lack of a temperature dependence in the millimeter wave conductivity between 20 K and 100 K makes hopping transport unlikely.

1. Introduction.

The α phase of di-[bis(ethylenedithiolo)tetrathiofulvalene]tri-iodine was the first organic material which showed highly conducting properties in two dimensions [1]. The nearly isotropic conductivity in the (ab)-plane is typically between 60 and 250 $(\Omega\text{cm})^{-1}$ at room temperature; $\sigma_b/\sigma_a \approx 2$ and $\sigma_b/\sigma_c \approx 4000$ [2]. The compound undergoes a metal insulator transition at $T_{MI} = 135$ K. A large number of studies have dealt with the nature of this phase transition [1-9], but very little progress has been made. The sudden opening of an energy gap was originally attributed to the formation of a charge density wave (CDW) [10]. Recently it was suggested that α-(BEDT-TTF)$_2$I$_3$ undergoes a transition to a spin density wave (SDW) ground state [11]. However, there are experimental results which contradict each of these explanations. The aim of this investigation was to study the electrodynamical response of α-(BEDT-TTF)$_2$I$_3$ in a wide frequency range at temperatures both above and below the phase transition. We will present field and frequency dependent transport measurements as well as studies of the dielectric behavior. First, we report on our X-ray studies and the search for superstructure reflections.

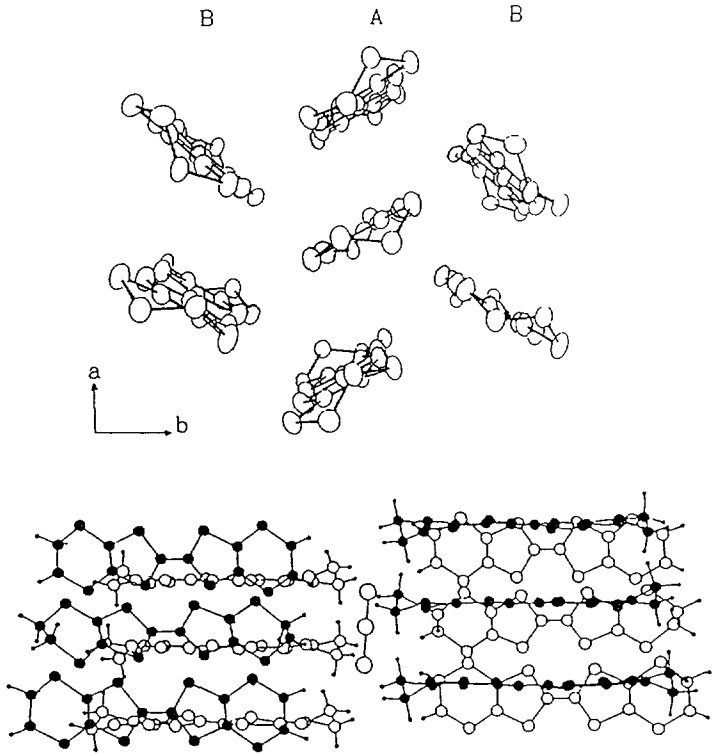

Fig. 1. — Crystal structure of α-(BEDT-TTF)$_2$I$_3$. The BEDT-TTF molecules are oriented along the c^* direction and stacked in two different chains. The (ab)-planes of the BEDT-TTF molecules are separated by I_3^- anions.

2. X-ray diffuse scattering investigations.

α-(BEDT-TTF)$_2$I$_3$ grows electrochemically in fairly large platelike ($5 \times 5 \times 0.1$ mm^3) dark-brown crystals with a smooth (ab)-surface of optical quality. The crystal structure is triclinic with a space group P$\bar{1}$. Each unit cell contains four BEDT-TTF molecules and two I_3 anions; therefore a 3/4 filled band is expected. From counting arguments, the charge carrier density can be estimated to be 1.16×10^{21} cm^{-3}. Hall effect and thermopower measurements indicate that holes carry the current in the high temperature range, while a change of sign is observed at T_{MI} [1, 2]. The organic cations form two crystallographically distinct stacks parallel to the a axis (Fig. 1a). One stack (A) consists of a series of dimer pairs (A and A') of BEDT-TTF molecules with faces parallel to each other. The molecules in the other stack (B) are uniformly spaced along the a axis, but tilted in an angle of 11° with respect to each other. The molecules in the two different stacks have dehedral angles of 59.4° and 70.4°, respectively. In addition to the face-to-face arrangement of the BEDT-TTF molecules within the stack, a side-by-side coupling between different stacks occurs, due to short (3.5 Å) interstack S$\cdots$S contacts compared to the somewhat large contacts within the stack. In the c^* direction, the planes of BEDT-TTF molecules are separated by layers of linear I_3^- anions which are oriented along the a axis (Fig. 1b).

The change in the transport properties at 135 K is not accompanied by a significant crystal-

lographic transition. Early studies showed that besides the usual contraction, the structural values at 100 K are not very different from those at room temperature and only minor changes in the crystal packing, dimerization and relative strengths of the interaction between neighboring BEDT-TTF molecules are reported [12-14]. It is considered unlikely that these changes are responsible for the metal-insulator transition, but it cannot be ruled out.

We performed temperature dependent X-ray diffuse scattering investigations of α-(BEDT-TTF)$_2$I$_3$ in order to look for the existence of superstructure reflections. As in previous studies of structural instabilities of organic conductors, the X-ray diffuse scattering experiment was performed with the so-called fixed film-fixed crystal method, using a monochromatized CuKα X-ray beam as incident radiation. Temperatures were regulated in the range from 30 K to room temperature. A single crystal having a platelet shape with the largest dimensions (3×1.5 mm^2) in the (ab)-plane was glued to a sample holder in good thermal contact with the cold finger of the cryocooler. The sample was oriented with respect to the X-ray beam in such a way that the (a^*, b^*) reciprocal plane was projected on the photographic film.

In addition to the Bragg reflections, room temperature X-ray patterns reveal intense diffuse lines belonging to H = const. layers of Bragg reflections. These diffuse lines, observed in the entire temperature range, are most likely due to disorder within the I_3-chains; this disorder is not correlated from chain to chain. X-ray patterns were taken on both sides of the metal-insulator phase transition. No superlattice reflections, which are the signature of a CDW ground state of low dimensional metals, could be detected below 135 K. Only an abrupt increase of intensity of several of the main Bragg reflections with odd Miller indices could be detected below this phase transition, in agreement with the findings of Nogami *et al.* [14]. Although our measurements allow us to rule out the formation of a CDW, they are unable to discriminate between the two opposite descriptions proposed for the structural modifications of the α-(BEDT-TTF)$_2$I$_3$ triclinic lattice at 135 K, namely: a dimerization of the stacks of inequivalent type of A and A′ molecules, breaking the inversion symmetry of the triclinic lattice [14], and an enhancement of the dimerization of the stacks of equivalent type B molecules, keeping the P$\bar{1}$ inversion symmetry [13].

3. Electrodynamic response.

3.1 FIELD DEPENDENT TRANSPORT. — We performed low frequency measurements by a standard four probe technique with 5 μm gold wires attached with silver paint to a pad of gold which was sputtered onto the surface of the sample. Each pad wrapped completely around the sample and both ends of the sample were covered with sputtered gold to ensure a homogeneous current injection. The applied electrical field was always kept below 1 mV/cm.

In an Arrhenius plot (Fig. 2) we show the conductivity of α-(BEDT-TTF)$_2$I$_3$ as a function of the inverse temperature. Below T_{MI} = 135 K the conductivity drops several orders of magnitude within a range of 10 K and indicates a first order phase transition. This is clearly confirmed by measurements of the specific heat [4, 9] and in agreement with thermal conductivity experiments [5], magnetic susceptibility experiments [6-8], and Bragg reflection measurements [14]. Below the phase transition the conductivity decreases with changing slope, indicating a temperature dependent gap or, more likely, strong mobility effects. At about 50 K we find a slope of approximately 0.025 eV. During several temperature sweeps around the phase transition we found no significant hysteresis.

The field dependent conductivity is displayed in figure 3a, where we have to note that $\sigma(E \rightarrow 0)$ is strongly temperature dependent. With decreasing temperature the deviation from Ohmic behavior can typically be observed at a lower field; however, in other samples temperature independent threshold fields were found as well. In order to avoid heating of the

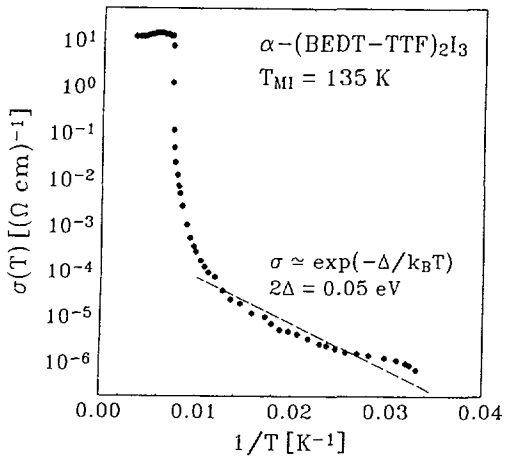

Fig. 2. — Arrhenius plot of the temperature dependent conductivity of α-(BEDT-TTF)$_2$I$_3$. Below the sharp drop at the metal insulator transition at T_{MI} = 135 K a temperature dependent gap opens. At around 50 K the slope is approximately 0.025 eV.

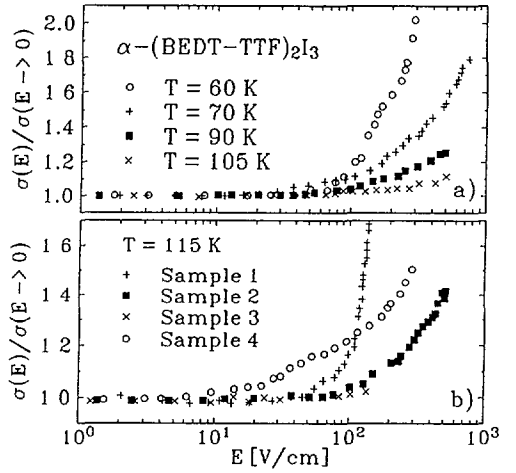

Fig. 3. — (a) Normalized conductivity as a function of applied electrical field for different temperatures. (b) The threshold and field dependence for non-linear conduction in α-(BEDT-TTF)$_2$I$_3$ varies from sample to sample between 1 V/cm and 80 V/cm (T = 115 K).

sample, short pulses were used at higher fields. The threshold field E_T is reproducible, but as shown in figure 3b, E_T and the non-linearity strongly depend on the sample. At 115 K we obtain values between 1 V/cm and 80 V/cm for the threshold field, and a conductivity enhancement between 4% and 70% at 150 V/cm. This may indicate a varying impurity concentration even within the same batch or dependence on the contacts.

3.2 MICROWAVE MEASUREMENTS. — Microwave and millimeter wave experiments in the temperature range from 4 K to 300 K were performed at 12, 35, 60 and 100 GHz using cylindrical TE_{011} resonant cavities [15, 16]. In general the sample was placed in the maximum of the

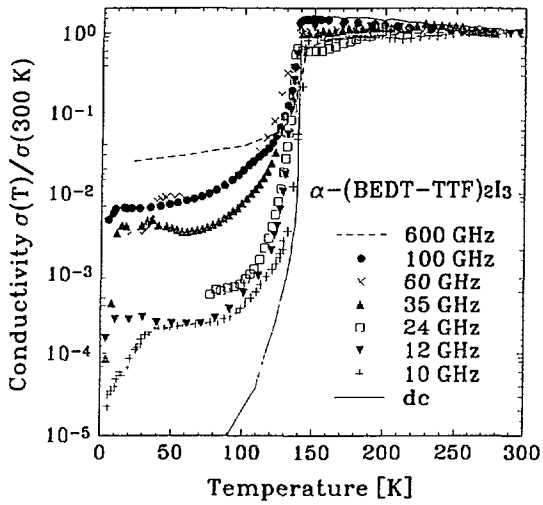

Fig. 4. — The temperature dependent conductivity of α-(BEDT-TTF)$_2$I$_3$ is shown for various frequencies in the millimeter and microwave range, together with the dc conductivity. The data at 600 GHz are taken from Železný *et al.* [20], the 24 GHz values were obtained by Mishima *et al.* [21]. While the dc conductivity steadily drops below the phase transition, the high frequency data show a temperature independent behavior. The plateau in the conductivity between 40 K and 100 K increases with increasing frequency.

electrical field with the current running in the highly conducting (ab)-plane. Measurements in the magnetic antinode with $\mathbf{H} \parallel c^*$ inducing eddy currents in the plane yielded the same results. The data were collected during warming and no hysteresis effects were observed. The complex conductivity $\hat{\sigma} = \sigma_1 + i\sigma_2$ was evaluated from the frequency shift and change in the quality factor between the loaded and the empty cavity using standard perturbation theory [17-19].

In figure 4 we display the temperature dependent conductivity of α-(BEDT-TTF)$_2$I$_3$ for different frequencies in the microwave and millimeter wave region, together with the dc curve, normalized to the room temperature values. The microwave data confirm the dc anisotropy, but the room temperature value is slightly smaller. For comparison, the reflection data [20] obtained in the submillimeter wave range (600 GHz) were included as well as microwave data from Mishima *et al.* [21] (24 GHz) and reference [22] (10 GHz). No significant frequency dependence was observed at 300 K. While in the metallic region the dc conductivity slightly increases with decreasing temperature and shows a broad maximum of twice the room temperature value at 140 K, the high frequency data are less temperature dependent than those at 10, 12 and 35 GHz. The slope of the high temperature conductivity increases with frequency and at 100 GHz it is similar to the dc curve. The same dependence was found by Przybylski *et al.* [10], and it was pointed out recently [21] that this may be a precursor effect of the metal-insulator transition which is much more pronounced in the b direction.

The phase transition at $T_{\mathrm{MI}} = 135$ K can be clearly seen from the microwave results as a drop in the conductivity of two to four orders of magnitude depending on the measurement frequency. After a sharp drop the conductivity becomes much less temperature dependent and smoothly saturates in a plateau. This regime of temperature independent conductivity continues down to about 20 K (varying somewhat from sample to sample). Note that this

plateau does not reflect the residual resistivity or the limit of the apparatus sensitivity, since at lower temperatures a further steep decrease of the conductivity is observed.

The most important point of the results displayed in figure 4 is that the absolute values of the low temperature conductivity plateau are frequency dependent. Between 10 GHz and 100 GHz the conductivity at 60 K increases almost two orders of magnitude. Qualitatively similar results were obtained for $\mathbf{E} \parallel a$ and $\mathbf{E} \parallel b$ in confirmation of reported results [3, 10, 21, 23].

3.3 OPTICAL EXPERIMENTS. — Using a Bruker IFS 113v rapid scan Fourier transform spectrometer, the infrared properties of α-(BEDT-TTF)$_2$I$_3$ single crystals were measured in both polarizations $\mathbf{E} \parallel a$ and $\mathbf{E} \parallel b$ at temperatures above and below the transition. The reflectance of the crystal surface was compared to a gold mirror at each temperature. The instrument covers the spectral range from 15 cm^{-1} to 5500 cm^{-1} and was operated with a 2 cm^{-1} resolution. The reflectivity for both polarizations is plotted in figure 5a. The results of our polarized reflection measurements confirm earlier observations [20, 24-28]. In agreement with the dc and microwave conductivity data the reflectivity in the b direction is significantly higher compared to $\mathbf{E} \parallel a$. The room temperature spectrum is dominated by a broad mid-infrared (MIR) peak at 2600 cm^{-1} due to an interband transition, and a Drude like edge at 4000 cm^{-1}. The broad transition is much less pronounced in the a direction, but apart from the absolute value the far-infrared (FIR) behavior shows the same features in the perpendicular direction. In the visible spectral range a strong dispersion appears near 20 000 cm^{-1} in the a direction, and it is assigned to molecular excitations of the tri-iodine anions [24, 26].

The temperature dependence of the reflectivity for $\mathbf{E} \parallel b$ is displayed in figure 6a. Below the phase transition at 135 K the reflectivity decreases and the much weaker MIR transition splits into two maxima at 2200 cm^{-1} and 2900 cm^{-1} This must be caused by a change in the band structure upon passing through T_{MI}. Although the crystal structure exhibits only minor changes in the crystal packing and relative strength of interaction between neighboring BEDT-TTF molecules, the dimerization in one of the stacks is more pronounced at low temperatures. This agrees with thermal expansion results, where a large anisotropic change at T_{MI} was also found [29].

3.4 DIELECTRIC RESPONSE. — In figure 7 the dielectric constant $\epsilon' = 1 - \sigma_2/\omega\epsilon_0$ is displayed over the entire frequency range. The low frequency data were obtained by measuring the out-of-phase component on a lock-in amplifier at various temperatures. The temperature dependence is shown in one inset of this Figure as well. The frequency dependence and large value of the dielectric constant $\epsilon'(\omega \to 0) = 5 \times 10^5$ indicate an overdamped low lying mode. In the second inset, which shows the optical part of ϵ' at $T = 60$ K on a linear scale, it can be seen that besides the feature at around 40 cm^{-1} the dielectric constant does not cross zero, but shows a minimum at 4000 cm^{-1} where the plasma frequency is expected to be.

4. Analysis and discussion.

4.1 OPTICS. — From the real and imaginary part of the low temperature conductivity as obtained by microwaves, the reflectivity R can be easily evaluated [30]. In the high temperature range α-(BEDT-TTF)$_2$I$_3$ exhibits a metallic conductivity where $\sigma_2 \ll \sigma_1$ and therefore $R \approx 1 - (8\epsilon_0\omega/\sigma_1)^{1/2}$ Figure 8 combines microwave, millimeter wave, and optical data as absorptivity $A = 1 - R$ *versus* frequency for both polarizations $\mathbf{E} \parallel a$ and $\mathbf{E} \parallel b$ at room temperature and at $T = 60$ K. The results of the two experimental methods match in both the insulating and metallic regimes.

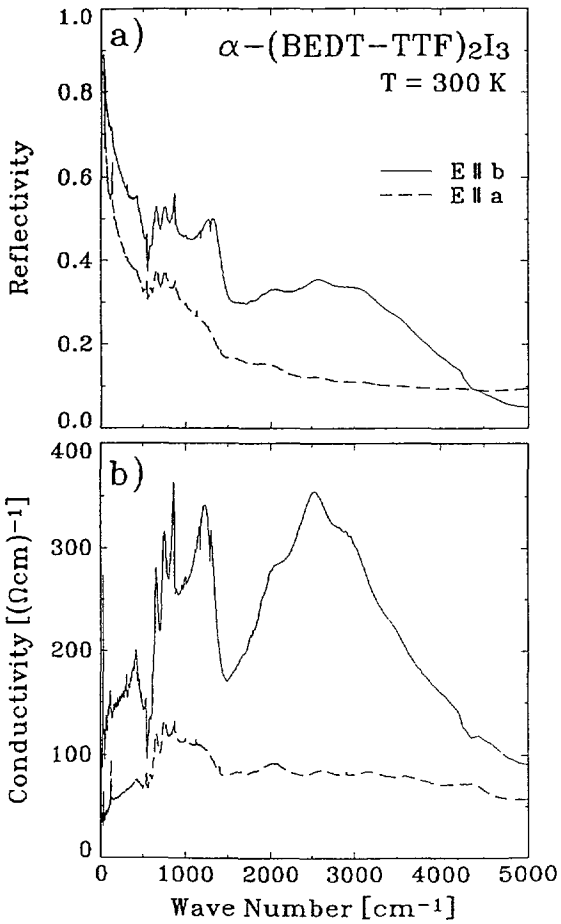

Fig. 5. — (a) Anisotropy of the room temperature reflectivity in the far and mid infrared spectral range. (b) The optical conductivity obtained from the Kramers-Kronig analysis of the reflectance data for both polarizations $\mathbf{E} \parallel a$ and $\mathbf{E} \parallel b$.

The anisotropy we observe within the plane is supported by calculations of the electronic band structure, but the results vary between different groups. From the overlap of the molecular orbitals estimated by the extended Hückel method, Mori *et al.* [31] found that the anisotropy in the (*ab*)-plane is not very large. Using a standard tight-binding approach, a semimetallic band structure was obtained, or more precisely a narrow-gap semiconductor which acts as a two-dimensional semimetal at higher temperatures due to the large thermal excitation of the conduction band [12, 31]. Basically the band structure remains unchanged at the phase transition, and is characterized by very narrow bands (approximately 0.3 eV) and a small direct gap (13 meV and 35 meV above and below T_{MI}, respectively).

In contrast to this, very recent band structure calculations indicate the existence of an essentially one-dimensional Fermi surface [32]. The Fermi surface consists of small pockets on the Brillouin zone boundary, which are two-dimensional in nature, but created from a one-dimensional Fermi surface crossing the Brillouin boundary. In agreement with this, recent MIR absorption measurements [33, 34] indicate a localization of charge in one of the two

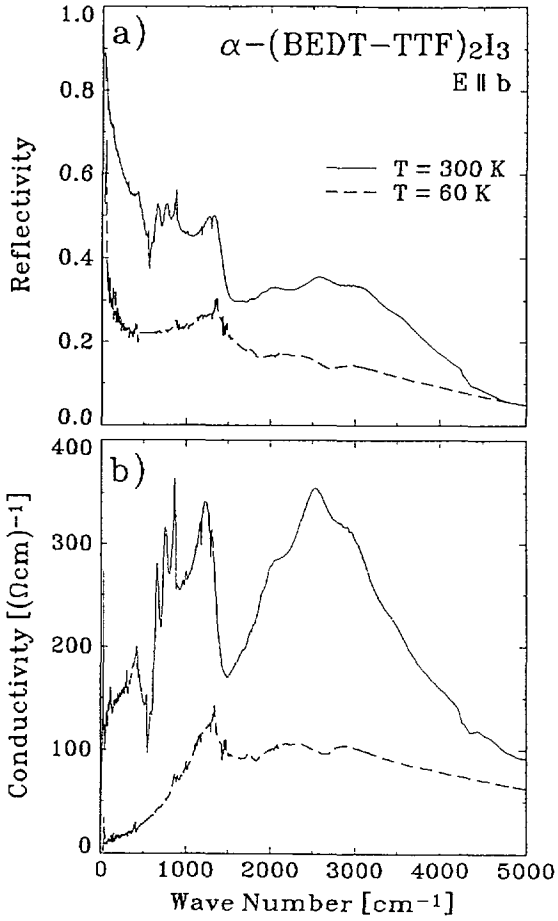

Fig. 6. — (a) Temperature dependence of the optical reflectivity of α-(BEDT-TTF)$_2$I$_3$ along the b axis. (b) Conductivity for T = 300 K and 60 K as a function of frequency.

different stacks of the donor molecules. This would imply that the crystals lose their quasi two-dimensional electronic properties below the phase transition and exhibit more quasi one-dimensional properties, since the coupling between neighboring stacks is reduced or lost. Our reflection measurements agree with this insofar as they show a much larger reduction in reflectivity for $\mathbf{E} \parallel b$ compared to the decrease for $\mathbf{E} \parallel a$. While in the high temperature phase the absorptivity (mainly in the FIR, but also in the MIR) is approximately twice as large for $\mathbf{E} \parallel a$ as it is for $\mathbf{E} \parallel b$, both are almost equal below T_{MI} (Fig. 8). However, the reflectance measurements as well as microwave data clearly show that α-(BEDT-TTF)$_2$I$_3$ is not a one-dimensional system below the phase transition as far as the conductivity is concerned. This is also supported by dc measurements [2] which indicate that the anisotropy changes only slightly while passing through the transition.

4.2 Frequency dependent conductivity. — In order to perform a Kramers-Kronig analysis, our IR data were combined with the data for the near infrared and visible range of Sugano *et al.* [26] and extrapolated as ω^{-4} at higher frequencies. At low frequencies the microwave

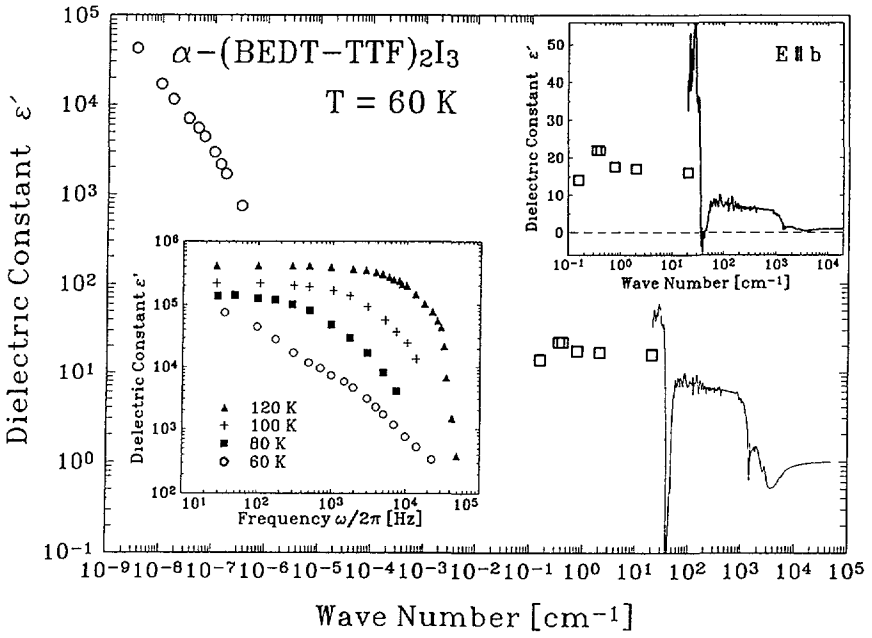

Fig. 7. — At $T = 60$ K the dielectric constant is plotted as a function of frequency. The upper right inset again shows the optical range on a linear scale indicating a zero crossing at 40 cm^{-1} and another minimum at about 4000 cm^{-1} where the plasma frequency is assumed. In the lower left inset the temperature dependence of the low frequency dielectric constant is displayed. Note the changed axis (3×10^{10} Hz = 1 cm^{-1})

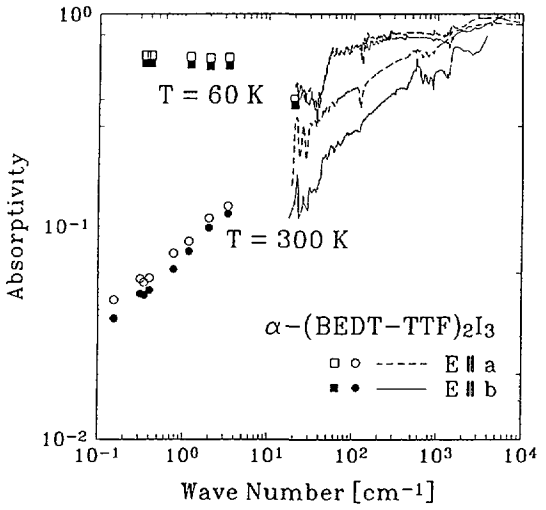

Fig. 8. — The absorptivity of α-(BEDT-TTF)$_2$I$_3$ in both polarizations $\mathbf{E} \parallel a$ and $\mathbf{E} \parallel b$ for temperatures above and below the metal-insulator transition. The microwave and millimeter wave results are shown as well.

Table I. — *Parameters of the Drude part obtained from a fit of the optical conductivity of α-(BEDT-TTF)$_2$I$_3$ at room temperature.*

	$\mathbf{E} \parallel a$	$\mathbf{E} \parallel b$
ν_p	3600 cm^{-1}	4600 cm^{-1}
$1/\tau$	3400 cm^{-1}	6000 cm^{-1}
ϵ_1	3.0	2.5
m_b/m_e	8.0	4.9
σ_{opt}	36 $(\Omega cm)^{-1}$	104 $(\Omega cm)^{-1}$

results were combined with the optical data. The zero frequency extrapolation was done in two ways: a the Hagen-Rubens behavior was used for $T > T_{MI}$, and a constant reflectivity was used for $T < T_{MI}$. The conductivity $\hat{\sigma}(\omega)$ was obtained with a Kramers-Kronig transformation [30] of the reflectivity data. The anisotropy of the room temperature conductivity of α-(BEDT-TTF)$_2$I$_3$ is shown in figure 5b. The optical conductivity leads to values comparable to the dc data: $\sigma_{opt}(\omega \to 0) = 104\ (\Omega cm)^{-1}$ and 36 $(\Omega cm)^{-1}$ for $\mathbf{E} \parallel b$ and $\mathbf{E} \parallel a$, respectively. We tried to separate the observed conductivity into a free electron contribution, which is described by a Drude behavior, and various interband and intraband transitions as well as phonon related contributions simulated by several Lorentz oscillators:

$$\hat{\epsilon}(\omega) = \epsilon_\infty + \frac{\omega_p^2}{\omega^2 - i\omega/\tau} + \sum_i \frac{\omega_{pi}^2}{\omega_{0i}^2 - \omega^2 - i\omega/\tau_i} \tag{1}$$

The parameters of the Drude part of the model as listed in table I are in good agreement with those of reference [25].

In the low temperature range (Fig 6), α-(BEDT-TTF)$_2$I$_3$ loses its metallic character, and a simple Drude fit is no longer suitable.

The excitation spectrum is dominated by MIR interband transitions and the plasma frequency derived from sum rule arguments

$$\int_0^{\omega_c} \sigma_1(\omega) d\omega = \frac{\epsilon_0 \pi \omega_p^2}{2} = \frac{ne^2}{2m_b} \tag{2}$$

is reduced to 3900 cm^{-1}, in agreement with the large Hall constant [2] and reduced ESR intensity [7, 8, 35]. While the room temperature data show a zero-crossing of the dielectric constant ϵ' at around 4000 cm^{-1}, at low temperatures a minimum is observed in this frequency range, but it does not cross zero (Fig. 7).

Figure 9 shows the frequency dependent conductivity at the two temperatures, one above and one below the phase transition, as determined from the Kramers-Kronig analysis. Since the results with $\mathbf{E} \parallel a$ are qualitatively similar, we will concentrate our discussions on the b-axis data. The room temperature data of microwave measurements [10] at 4.6, 9.3 and 23.5 GHz are included in the figure and an excellent agreement is found. While the conductivity is only slightly frequency dependent in the metallic regime ($T > 135$ K), below the phase transition a strong frequency dependence can be seen at low frequencies. We do not find a resonance-like

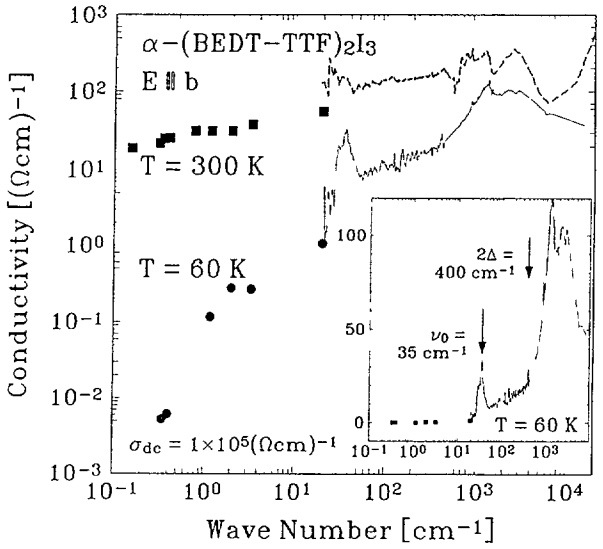

Fig. 9. — Frequency dependent conductivity at $T = 60$ K and $T = 300$ K. The inset enhances the single particle gap at 400 cm^{-1} The peak at 35 cm^{-1} is discussed in the text.

feature in the conductivity between 10 and 600 GHz as has been found previously in compounds which develop a CDW or SDW ground state [36]. The linear plot in the inset of figure 9 clearly indicates an energy gap 2Δ at around 400 cm^{-1} = 0.05 eV. This gaplike feature agrees with the activation energy (2Δ = 0.05 eV) obtained from dc resistivity measurements (Fig. 2). This is also in good agreement with the energy gap derived from the mean field theory, and $2\Delta/k_BT_{MI} = 4.2$.

At 35 cm^{-1} a large conductivity peak with a width of only 10 cm^{-1} can be seen (Fig. 9). Although a small feature can be recognized at room temperature, a strong enhancement occurs below the transition temperature, in agreement with the submillimeter wave data of reference [20]. This change and gradual disappearance above T_{MI} indicates a coupling to the free carriers and screening of the phonon effective charge. The strength of this mode is approximately the same for $\mathbf{E} \parallel a$ as it is for $\mathbf{E} \parallel b$. It may be attributed to the fundamental vibration $\nu_{54}(b_{2u})$ of the BEDT-TTF molecule; this mode was calculated to be IR and Raman active near 40 cm^{-1} at $T = 300$ K. Železný *et al.* [20] assigned their feature at 31 cm^{-1} to an IR active external vibration of the entire (BEDT-TTF)$_2$I$_3$. Furthermore resonant Raman scattering experiments show similar features around 30 cm^{-1}, which have been attributed to the librational mode of the tri-iodine anion [37, 38]. A similar assignment was made for third-order optical susceptibility results from femtosecond four-wave mixing experiments [39]. However, we would not expect to observe a mode of the same intensity in both directions. Recent low temperature Raman experiments [40, 41] report a strong mode at 30 cm^{-1} and a weaker one at 38.5 cm^{-1}. The authors assign both features to librations of the BEDT-TTF molecule. After transforming α-(BEDT-TTF)$_2$I$_3$ into superconducting α_t-(BEDT-TTF)$_2$I$_3$ by annealing the crystal several days at around 80 °C, these modes disappear upon entering the superconducting state at $T < T_c = 8.1$ K. A very similar behavior was observed in $NbSe_3$, where a CDW mode at 30 cm^{-1} vanishes below T_c [42]. In the case of α-(BEDT-TTF)$_2$I$_3$, however, the 35 cm^{-1} peak is clearly not a CDW mode. It is likely to be a phonon peak but the final assignment remains unclear.

The high ac conductivity at low temperatures (Fig. 4) may be explained by hopping transport between localized impurity states in the energy gap. As expected for non-linear and hopping processes, the overall frequency dependence of the conductivity at 60 K (Fig. 9) is dominated by a $\sigma \propto \omega^s$ behavior, where in our case $s \approx 1.3$. Neither the standard equation [43] for variable range hopping nor photon assisted hopping describe our experimental results well, and a phenomenological explanation must lie between the two as far as the frequency dependence is concerned. However, in contrast to the experimental findings between 40 K and 100 K, a temperature dependence of the ac conductivity is expected. Below 40 K these states freeze out since the Fermi level drops. Heavy iodine doping leads to an increase of the microwave conductivity between 50 K and 100 K [23]; the drop and subsequent plateau seen in the conductivity are smoothed out with increased doping and finally a constant slope is observed in the entire low temperature range below 135 K. Studies on pressed α-(BEDT-TTF)$_2$I$_3$ powder also show the absence of the plateau, and the microwave conductivity steadily decreases over the entire temperature range [44]. These findings strongly indicate that in the pure specimens the high frequency conductivity is not governed by hopping processes.

4.3 NON-LINEAR TRANSPORT. — Field dependent transport can be explained with a variety of mechanisms; among the most likely are non-linear contributions due to hopping or a sliding CDW or SDW. Carrier heating can be ruled out since conductivity and therefore the mobility is low. Most models predict a dependence of the threshold field on the impurities of the crystal. In the case of density waves [36], the threshold field $E_T \propto n_i$ or n_i^2 for strong and weak pinning, respectively. This can explain the change of threshold field from sample to sample, but no systematic study of the impurity dependence of the threshold field of α-(BEDT-TTF)$_2$I$_3$ has been performed yet.

Various models for density waves [36] relate the threshold field of the non-linear conduction to the static dielectric constant, since both are caused by the same microscopic mechanism:

$$E_T \epsilon_0 \epsilon'(\omega \to 0) = c 2 e n_\perp, \tag{3}$$

with c a numerical constant that is expected to be at the order of unity and has been eperimentally verified in a large number of CDW materials. Using $n_\perp \approx 10^{14}$ cm^{-2} as the number of conducting chains per unit area in α-(BEDT-TTF)$_2$I$_3$ we obtain with $c \approx 0.05$ a much smaller value. Recently, however, Trætteberg *et al.* [45] found a similar discrepancy ($c = 0.02$) in TMTSF alloys.

Models for non-linearities based on a single particle picture for electrons depend critically on the amplitude of the energy gap at the Fermi level. The strong temperature dependence of the dc activation energy, assuming it is not solely caused by decreasing mobility, would therefore imply a temperature dependent threshold field which in our experiments was not found in general. However, single particle conduction cannot be ruled out at this point, though it is usually observed at higher fields. Hopping conduction leads to non-linear transport and does not automatically imply a temperature dependent threshold field.

4.4 DIELECTRIC BEHAVIOR. — The static dielectric constant can be calculated by the standard expression:

$$\epsilon'(\omega \to 0) = 1 + \frac{\hbar^2 \omega_p^2}{6\Delta^2}. \tag{4}$$

Using $\omega_p(T = 300\ \text{K})$ for the plasma frequency we obtain $\epsilon'(\omega \to 0) \approx 88$. The plasma frequency at low temperatures is approximately the room temperature value, which puts ϵ' in agreement with the microwave results. The large dielectric constant at low frequencies indicates

an additional low lying contribution and its frequency dependence infers an overdamped mode. Close to the metal-insulator transition at $T = 120$ K, it is almost critically damped as indicated by the sharp drop of ϵ' at around 5×10^4 Hz. With decreasing temperature it moves to lower frequencies and broadens significantly. Such behavior was widely observed in density wave materials [36] and also in various glasses and random systems [46].

The dielectric constant shows a zero crossing around 40 cm^{-1} and a strong peak below that, which is related to the narrow mode at 35 cm^{-1} (Fig. 7). One might assume this mode is the phason mode of a pinned CDW or SDW, but the relatively small ϵ' in the microwave and millimeter wave range of approximately 20 compared to the low frequency values of 2×10^5 indicates that the main excitations are at lower frequencies.

5. Summary.

Some of the experimental findings on α-(BEDT-TTF)$_2$I$_3$ show similarities to TTF-TCNQ, which undergoes a CDW phase transition at 54 K. Although transport experiments never clearly exhibited collective phenomena, X-ray and high pressure transport investigations undoubtedly show the formation of a CDW in TTF-TCNQ. The metal-insulator transition in α-(BEDT-TTF)$_2$I$_3$, however, is not due to the formation of a CDW ground state. X-ray scattering experiments indicate that there is no superstructure below $T_{\mathrm{MI}} = 135$ K. This is supported by our high frequency conductivity data where no resonance in the millimeter wave range was found as can usually be seen in a CDW material as a feature of the pinned mode. In order to describe the contribution of the pinning [47], a phason term $\frac{ne^2}{\epsilon_0 m^* \omega_0^2}$ has to be added to equation (4). With $m^* = 1000 m_b$ as a typical value for CDW systems [36], the pinning frequency ω_0 can be estimated to be 3.3 cm^{-1} = 100 GHz. This is in contrast to the experimental data. Another independent confirmation comes from the dielectric constant: the large $\epsilon'(T \to 0)$ decreases below 10^5 Hz where strong contributions from the internal deformations and pinned mode of a CDW are still expected. The microwave dielectric constant was measured to be only 20 while it is about 10^5 in CDW compounds [36].

An interesting possibility was recently pointed out by Hasegawa and Fukuyama [11] in order to explain findings of an anomalous magnetoresistance seen by Kajita *et al.* [32, 48]. The application of pressure affects the metal-insulator transition of α-(BEDT-TTF)$_2$I$_3$ in two different ways. First, the temperature of the phase transition decreases linearly with applied pressure up to approximately 12 kbar where a transition is no longer seen in the resistivity for $T > 1.3$ K. Secondly, pressurized samples show a finite conductivity on the low temperature side of the transition, increasing as a function of pressure. If an external magnetic field is applied in this situation ($p = 14.7$ kbar), the metal insulator transition is reestablished at about 60 K. Hasegawa and Fukuyama now suggest that this anomalous magnetoresistance can be understood by a field induced spin density wave (FISDW) due to an almost nested quasi-one-dimensional Fermi surface, although the magnetic field of 0.2 Tesla is much smaller than that in (TMTSF)$_2X$ compounds (ca. 10 Tesla) which typically exhibit a transition at 10 K. This interpretation is in contrast to the results of magnetization measurements on α-(BEDT-TTF)$_2$I$_3$. The paramagnetic susceptibility χ at room temperature is larger than the value inferred from the Pauli susceptibility of a non-interacting electron gas. It decreases slowly above the phase transition T_{MI} where it drops sharply. No sign of anisotropy was found, and over the entire temperature range the spin susceptibility has an identical temperature dependence in all directions. In agreement with the transport measurements the application of pressure shifts the drop of the susceptibility to lower temperatures without changing the overall behavior [6, 7]. At temperatures below the transition α-(BEDT-TTF)$_2$I$_3$ becomes diamagnetic in all directions,

indicating that the compound has a non-magnetic ground state. NMR experiments on powder samples [49] show a steady decrease of the relaxation rate T_1^{-1} in the entire temperature range and no indications of a SDW transition.

Since there are no indications for a transition to a CDW or SDW ground state, it becomes more likely that the large change in the electrodynamic response is caused by the small structural variations at the phase transition. They are responsible for a change in the charge distribution within the molecule, the dimerization, and the interaction between neighboring BEDT-TTF molecules. The result of the IR reflectivity and absorption [33, 34] point in this direction, as do thermal expansion measurements [29].

Hopping mechanisms are a widely used approach to describe the frequency dependent conductivity in the audio frequency. But a number of our experimental results on the non-linear and frequency dependent transport are in contrast to simple hopping theories: the low threshold field, the lack of a temperature dependence between 20 K and 100 K in the microwave and millimeter wave range, and the monotonic increase of the conductivity up to the optical range, to name just a few. However, at this point single particle hopping transport cannot be ruled out.

In conclusion, below the metal-insulator phase transition at 135 K, α-(BEDT-TTF)$_2$I$_3$ shows a frequency dependent conductivity in the microwave and millimeter wave spectral range and a large dielectric constant at low frequencies. The transport becomes non-linear at higher electrical field with a smooth onset. The anomalous transport properties in the low temperature regime cannot easily be explained by single particle hopping conduction between impurity states. But there is clearly no formation of a CDW in α-(BEDT-TTF)$_2$I$_3$ since no signs of a superstructure were found in X-ray scattering experiments. A recent suggestion [11] that α-(BEDT-TTF)$_2$I$_3$ develops a SDW ground state at 135 K is faced by the results of magnetic susceptibility measurements which show a completely diamagnetic phase below the transition regardless the orientation and application of pressure [7]. The nature of the metal-insulator phase transition at 135 K remains unresolved, but it does not seem to be a Fermi surface instability.

Acknowledgments.

We thank S. Cho for performing some of the low frequency measurements. One of us (M.D.) would like to thank the Alexander von Humboldt-Foundation for support.

References

[1] Bender K., Hennig I., Schweitzer D., Dietz K., Endres H. and Keller H. J., *Mol. Cryst. Liq. Cryst.* **108** (1984) 359.

[2] Pokhodnya K. I., Sushko Y. V. and Tanatar M. A., *Sov. Phys. JETP* **65** (1987) 795.

[3] Bender K., Dietz K., Endres H., Helberg H. W., Hennig I., Keller H. J., Schäfer H. W. and Schweitzer D., *Mol. Cryst. Liq. Cryst.* **107** (1984) 45.

[4] Hennig I., Diploma thesis, Univ. Heidelberg (1985).

[5] Hennig I., Bender K., Schweitzer D., Dietz K., Endres H., Keller H. J., Gleitz A. and Helberg H. W., *Mol. Cryst. Liq. Cryst.* **119** (1985) 357.

[6] Merzhanov V. A., Kostyuchenko E. E., Faber O. E., Shchegolev I. F. and Yagubskii E. B., *Sov. Phys. JETP* **62** (1985) 165.

[7] Rothaemel B., Forró L., Cooper J. P., Schilling J. S., Weger M., Bele P., Brunner H., Schweitzer D. and Keller H. J., *Phys. Rev. B* **34** (1986) 704.

[8] Sugano T., Saito G. and Kinoshita M., *Phys. Rev. B* **34** (1986) 117.

[9] Fortune N. A., Murata K., Ishibahi M., Tokumoto M., Kinoshita N. and Anzai H., *Solid State Commun.* **77** (1991) 265.

[10] Przybylski M., Helberg H. W., Schweitzer D. and Keller H. J., *Synth. Met.* **19** (1987) 191.

[11] Hasegawa Y. and Fukuyama H., *Physica B* **184** (1993) 498.

[12] Emge T. J., Leung P. C. W., Beno M. A., Wang H. H. and Williams J. M., *Mol. Cryst. Liq. Cryst.* **138** (1986) 393.

[13] Endres H., Keller H. J., Swietlik R., Schweitzer K. A. D. and Krüger C., *Z. Naturforsch.* **41a** (1986) 1319.

[14] Nogami Y., Kagoshima S., Sugano T. and Saito G., *Synth. Met.* **16** (1986) 367.

[15] Donovan S., Klein O., Dressel M., Holczer K. and Grüner G., *Int. J. Infrared and Millimeter Waves* **14** (1993) 2459.

[16] Dressel M., Klein O., Donovan S. and Grüner G., *Int. J. Infrared and Millimeter Waves* **14** (1993) 2489.

[17] Buranov L. I. and Shchegolev I. F., *Prib. Tekh. Eksp. (Engl.)* **14** (1971) 528.

[18] Schäfer H., Ph.D. thesis, Univ. Göttingen (1983).

[19] Klein O., Donovan S., Dressel M. and Grüner G., *Int. J. Infrared and Millimeter Waves* **14** (1993) 2423.

[20] Želzný V., Petzelt J., Swietlik R., Gorshunov B. P., Volkov A. A., Kozlov G. V., Schweitzer D. and Keller H. J., *J. Phys. France* **51** (1990) 869.

[21] Mishima T., Kajita K., Kanke O., Nishio Y., Kobayashi H., Kobayashi A., Kato R. and Kobayashi M., *Synth. Met.* **56** (1993) 2262.

[22] Dressel M., *Ph.D. thesis, Univ. Göttingen, 1989.*

[23] Kremer W., Helberg H. W., Gogu E., Schweitzer D. and Keller H. J., *Ber. Bunsenges. Phys. Chem.* **91** (1987) 896.

[24] Koch B., Geserich H., Ruppel W., Schweitzer D., Dietz K. H. and Keller H. J., *Mol. Cryst. Liq. Cryst.* **119** (1985) 343.

[25] Kaplunov M. G., Yagubskii E. B., Rosenberg L. P. and Borodko Y. G., *Phys. Stat. Sol. (a)* **89** (1985) 509.

[26] Sugano T., Yamada K., Saito G. and Kinoshita M., *Solid State Commun.* **55** (1985) 137.

[27] Meneghetti M., Bozio R. and Pecile C., *J. Phys. France* **47** (1986) 1377.

[28] Yakushi K., Kanabara H., Tajima H., Kuroda H., Saito G. and Mori T., *Chem. Lett.* **60** (1987) 4251.

[29] Heidmann C.-P., Barnsteiner A., Groß-Alltag F., Chandrasekhar B. S. and Hess E., *Solid State Commun.* **84** (1992) 711.

[30] Wooten F., Optical Properties of Solids (Academic Press, San Diego, 1972).

[31] Mori T., Kobayashi A., Sasaki Y., Kobayashi H., Saito G. and Inokuchi H., *Chem. Lett.* **1984** (1984) 957.

[32] Orjiro T., Kajita K., Nishio Y., Kobayashi H., Kobayashi A., Kato R. and Iye Y., *Physica B* **184** (1993) 494.

[33] Moldenhauer J., Pokhadnia K., Schweitzer D. and Keller H. J., *Synth. Met.* **56** (1993) 2554.

[34] Moldenhauer J., Horn C., Pokhadnia K., Schweitzer D., Heinen I. and Keller H. J., *Synth. Met.* **60** (1993) 31.

[35] Venturini E. L., Azevendo L., Schirber J. E., Williams J. M. and Wang H. H., *Phys. Rev. B* **32** (1985) 2819.

[36] Grüner G., *Rev. Mod. Phys.* **60** (1988) 1129.

[37] Sugai S. and Saito G., *Solid State Commun.* **58** (1986) 759.

[38] Świetlik R., Schweitzer D. and Keller H. J., *Phys. Rev. B* **36** (1987) 6881.

[39] Trùòng K. D., Grenier P., Houde D. and Bandrauk A. D., *Chem. Phys. Lett.* **196** (1992) 280.

[40] Pokhodnia K. I., Graja A., Weger M. and Schweitzer D., *Z. Phys. B* **90** (1993) 127.

[41] Graja A., *Synth. Met.* **56** (1993) 2477.

[42] Sooryakumar R. and Klein M., *Phys. Rev. Lett.* **45** (1980) 660.

[43] Mott N. F. and Davis E. A., Electronic Processes in Non-Crystalline Materials, 2 ed. (Clarendon, Oxford, 1975).

[44] Müller G., Helberg H. W., Schweitzer D. and Keller H. J., *Synth. Met.* **41-43** (1991) 1999.

[45] Trætteberg O., Kriza G., Lenoir C., Huang Y. S., Batail P. and Jérome D., *Synth. Met.* **56** (1993) 2785.

[46] Ngai K. L., *Comments Solid State Phys.* **9** (1979/80) 127 and 141.

[47] Lee P. A., Rice T. M. and Anderson P. W., *Solid State Commun.* **14** (1974) 703.

[48] Kajita K., Ojiro T., Fujii H., Nishio Y., Kobayashi H., Kobayashi A. and Kato R., *J. Phys. Soc. Jpn.* **61** (1992) 23.

[49] Hennig I., Ph.D. thesis, Univ. Heidelberg (1989).